The Journal of Analysis (2020) 28:1009–1022
https://doi.org/10.1007/s41478-020-00230-4

ORIGINAL RESEARCH PAPER

Compressible fluid film lubrication of rollers with thermal effects

N. Jalatheeswari[1] · Dhaneshwar Prasad[1]

Received: 14 October 2019 / Accepted: 13 February 2020 / Published online: 25 February 2020

Abstract

The present paper squarely aims to analyze the squeezing velocity of a hydrodynamic lubrication used for symmetric roller bearings. Hydrodynamic compressible fluid film lubrication of cylindrical rollers is here considered under the influence of non Newtonian power law lubricants with squeezing velocity and cavitations. The changes that show up in lubrication consistency due to pressure, density and temperature are shown via ures and tables. Further, pressure, density, temperature, load, traction and coefficient of traction for various consistency index n and normal speeds are calculated and compared with the previous results. Those results are united with the previous findings.

Keywords Compressible fluid · Adiabatic · Power-law · Lubrication · Roller bearings · Squeezing velocity · Consistency

Mathematics Subject Classification 76N10

List of symbols

α Pressure coefficient
β Temperature coefficient
h Film thickness
h_0 Minimum film thickness
m Lubricant consistency
m_0 Consistency at ambient pressure and temperature
p Hydrodynamic pressure

This paper is presented in the RMS conference held in August 1–3, 2019 at Pondicherry University and selected as **BEST PAPER AWARD**.

✉ N. Jalatheeswari
njalatheeswari@gmail.com

Dhaneshwar Prasad
rpdhaneshwar@gmail.com

[1] Kanchi Mamunivar Centre for Post Graduate Studies, Pondicherry, India

q Squeezing parameter
R Radius of cylinder
T Lubricant temperature
T_0 Ambient temperature
T_{Fh} Traction force
u Velocity of the lubricant in x-direction
U Velocity of the lubricant at $y = h/2$
v Velocity of the lubricant in y-direction
V Normal velocity (V/2) of either cylinder
x_1 Point of maximum pressure
x_2 Cavitation point

1 Introduction

Nature teaches human many valid techniques at free of cost, and lubrication is one of such techniques. For example, saliva plays the role of a lubricant when it comes to eschewing the given solid food. Today, the industries do function in automatic mode because at instances, the industries have to work all the twenty four hours without a break. The application of lubricant for smooth running of machine was successful with some lacunae like acid etching, formation of debris in lubricant. And with bearing defects like surface roughness, waviness, race misalignment, formation of micro pits, etc were reported [1].

The earlier Reynolds equation for the study of incompressible and isoviscous fluid gave fruitful results only in case of low pressure, and altogether ignored the density and viscosity variation. In order to manage the load system, different lubricants were utilized. Newtonian lubricant is the well known simple lubricant used to attend the shear stress and shear strain rate. However, the Newtonian lubricant is not successful for the calculation of traction force. Non-Newtonian lubricant is nothing but inclusion of concentration to the base oil. The Power law fluid model is one among them, and is highly successful in the study of squeeze films, externally pressurized bearings, conical and roller bearings including Newtonian as well.

Floberg and Jakobsson [2] gave forth an able mass conserving algorithm to examine the lubricant film with cavitations. The algorithm exploits ad-hoc equations to detect the cavitations boundaries. Further, it assigns fixed pressure value to passive area and thereby makes Reynolds equation a successful one. Elrod and Adams [3] pioneered the development of such cavitations algorithm. Here, detection of cavitations boundary does not arise due to the use of simple equation. To the passive region they launched a switch function g(p), where g(p) stands one when pressure is more than the cavity pressure, and zero otherwise. Likewise, the Poiseuille term of Reynolds equation could be unnaturally brought down in the domain of cavitation. Here, EHL and dynamic transient behavior respond to well with outputs in the study of lubrication problems [4].

In order to establish the active and cavitated film domain, previously complementary concept was used. Cavitation related problems were extensively

used by many authors, like Lewy and Stampacchia [5], Rohde and McAllister [6], Cimatti [7]. Strozzi [8] proposed a piquant model of decoding the resumptions pertaining to cavitation. Then Kostreva [9], Oh [10] and Oh and Goenka [11] widely used the issue of cavitation for hydrodynamic and EHL. They found a solution to active and cavitated film regions adopting complementarity but not for conservation of mass. This exception arises because Reynolds equations are worked out for assuming a constant lubricant density. Even this presumption is permissible in active region but in the passive regions the density definitely changes in space and time. Giacopini et al. [12] demonstrated how the adoption of constant fluid density may lead to false serving of film reformation.

Further, different level of study of EHL has contributed to the augment of longevity of the contraption. So far only a little contribution is disclosed in the field of lubricating performance of finite line contact which provided unsteady conditions. Kushwaha and Rahnejat [13] explained the character of finite line EHL of rolling contacts under transient conditions. Here, the load is allowed to vary from time to time. The variation is performed by the transient load at the background of lubrication. The lubricant fluid present at the place of contact affects both the pressure and the film thickness there. Along with finite line contacts subject to transient load conditions they also clarified film thickness and pressure variations in the lubricated system [14]. This system further motivates us to study of the lubricated finite line contacts.

In continuation to the above discussion, this paper includes the analysis of changes in hydrodynamic pressure and temperature of non Newtonian power law lubricants beneath the rigid symmetrical cylindrical rollers with cavitations and normal squeezing motions. The consistency equation for compressible fluids is considered to be functions of the one dimensional pressure and temperature under isothermal boundaries. The normal load carrying capacity and the traction force are calculated for the various values of the consistency index and normal squeezing parameter (Fig. 1).

2 Mathematical analysis

Considering the basic fluid flow momentum [15] and continuity equations [16] of symmetric cylinders for compressible power law fluid may be written as:

$$\frac{dp}{dx} = \frac{\partial \tau}{\partial y} \tag{1}$$

$$\frac{\partial (\rho u)}{\partial x} + \frac{\partial (\rho v)}{\partial y} = 0 \tag{2}$$

The Heat Energy equation considered to be [17]

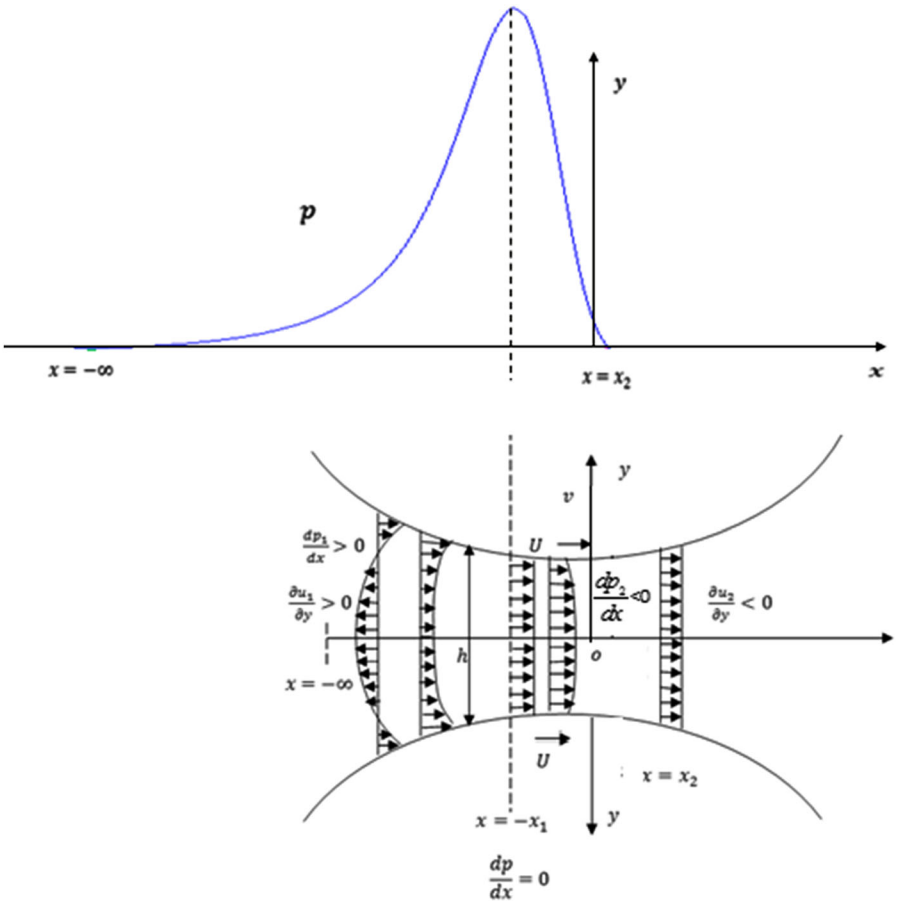

Fig. 1 Lubrication of symmetric cylindrical rollers

$$\rho\, c_p\, u\, \frac{dT}{dx} = \tau \frac{\partial u}{\partial y} + \varepsilon\, T\, u \frac{dp}{dx} \tag{3}$$

Here c_p is the specific heat of the lubricant at constant pressure and the density $\rho$is calculated by [18].

$$\rho = 1 + \frac{0.6 \times 10^{-9} p}{1 + 1.7 \times 10^{-9} p}$$

The shear stress and the strain rate relation for non-Newtonian power law fluids is:

$$\tau = m \left| \frac{\partial u}{\partial y} \right|^{n-1} \frac{\partial u}{\partial y} \tag{4}$$

The consistency m is assumed to vary as follow as

$$m = m_0\, e^{\alpha p + (T_0 / T)} \tag{5}$$

where p and T are hydrodynamics pressure and temperature respectively. Considering the boundary conditions for the given system as:

$$\frac{\partial u}{\partial y} = 0 \; at \; y = 0; u = U at \; y = \frac{h}{2}; \; T = T_{01} \; at \; x = -\infty; \tag{6}$$

Integrating Eq. (1) with respect to 'y' with the above boundary conditions gives

$$u_1 = U + \left[\frac{1}{m}\left(\frac{dp_1}{dx}\right)\right]^{\frac{1}{n}}\left[\frac{n}{n+1}\left(y^{\frac{n+1}{n}} - \left(\frac{h}{2}\right)^{\frac{n+1}{n}}\right)\right]; -\infty < x \leq -x_1 \tag{7}$$

Similarly, for the region $-x_1 \leq x \leq x_2$, one can have

$$u_2 = U - \left[\frac{1}{m}\left(-\frac{dp_2}{dx}\right)\right]^{\frac{1}{n}}\left[\frac{n}{n+1}\left(y^{\frac{n+1}{n}} - \left(\frac{h}{2}\right)^{\frac{n+1}{n}}\right)\right] : -x_1 \leq x \leq x_2 \tag{8}$$

Integration of the continuity Eq. (2) with the boundary conditions together with the specified conditions: $v_{h/2} = \frac{U}{2}\frac{dh}{dx} + \frac{V}{2}$ and $v_0 = 0$, gives

$$\frac{\partial}{\partial x}\rho \int_0^{h/2} u\, dy = -\frac{\rho V}{2} \tag{9}$$

Further integration of the above equation with the associated conditions:
$\frac{dp_1}{dx} = 0$ at $x = -x_1$ and $h = h_1$, one can get

$$\frac{dp_1}{dx} = m\left(\frac{2n+1}{n}\right)^n\left(\frac{2}{h}\right)^{2n+1}\left[\frac{r_1}{\rho} + \frac{Uh}{2}\right]^n; -\infty < x \leq -x_1 \tag{10}$$

Similarly for the other region

$$\frac{dp_2}{dx} = -m\left(\frac{2n+1}{n}\right)^n\left(\frac{2}{h}\right)^{2n+1}\left[-\left(\frac{r_2}{\rho} + \frac{Uh}{2}\right)\right]^n; -x_1 \leq x \leq x_2 \tag{11}$$

Making the above equations dimensionless, these Eqs. (10) and (11) are reduced to

$$\frac{d\overline{p_1}}{d\overline{x}} = \frac{\overline{m}\,\overline{f}^n}{\overline{h}^{2n+1}}; -\infty < \overline{x} \leq -\overline{x_1} \tag{12}$$

$$\frac{d\,\overline{r_1}}{d\,\overline{x}} = \overline{\rho_1}\;\overline{q}; -\infty < \overline{x} \leq -\overline{x_1} \tag{13}$$

$$\frac{d\overline{p_2}}{d\overline{x}} = -\frac{\overline{m}\,\overline{g}^n}{\overline{h}^{2n+1}}; -\overline{x_1} \leq \overline{x} \leq \overline{x_2} \tag{14}$$

$$\frac{d\overline{r_2}}{d\overline{x}} = \overline{\rho_2}\ \overline{q}; -\overline{x_1} \le \overline{x} \le \overline{x_2} \tag{15}$$

Where

$$\overline{f} = (\overline{r_1}/\overline{\rho}) + (\overline{h}/2); \overline{g} = -\left[(\overline{r_2}/\overline{\rho}) + (\overline{h}/2)\right]; \overline{\rho} = 1 + \frac{0.6 \times 10^{-9}\,\overline{p}}{1 + 1.7 \times 10^{-9}\,\overline{p}};$$

$$\overline{h} = \frac{h}{h_0};\ \overline{p} = \alpha p;\ \overline{E} = e^{\overline{p} + (\overline{T_0}/\overline{T})};\ c_n = \left(\frac{4(2n+1)}{n}\right)^n \sqrt{\frac{2R}{h_0}} \left(\frac{U}{h_0}\right)^n;\ \overline{T} = \beta T\ ;$$

$$\overline{r} = \frac{r}{\rho_0\, U\, h_0}; \overline{q} = \frac{V}{2U}\sqrt{\frac{2R}{h_0}}; \overline{\gamma} = \frac{\beta}{\rho_0 C_p \alpha}; \overline{\varepsilon} = \varepsilon\ /\beta;$$

Making the above equation dimensionless, it reduces to

$$\frac{d\overline{T_1}}{d\overline{x}} = \frac{\overline{m}\,\overline{f}^n\,\overline{\gamma}}{\overline{\rho}\,\overline{h}^{2n+1}}\left(\overline{\varepsilon}\overline{T_1} - \frac{\overline{\rho}\overline{h}}{2\overline{r_1}} - 1\right); -\infty < \overline{x} \le -\overline{x_1} \tag{16}$$

$$\frac{d\overline{T_2}}{d\overline{x}} = -\frac{\overline{m}\,\overline{g}^n\,\overline{\gamma}}{\overline{\rho}\,\overline{h}^{2n+1}}\left(\overline{\varepsilon}\overline{T_2} - \frac{\overline{\rho}\overline{h}}{2\overline{r_2}} - 1\right); -\overline{x_1} \le \overline{x} \le \overline{x_2} \tag{17}$$

Making the above Eqs. (7) and (8) dimensionless, they reduce to

$$\overline{u_1} = 1 + 2^{\frac{1}{n}}\left(\frac{4\,(2n+1)}{n+1}\right)\frac{\overline{f}}{\overline{h}^{\frac{2n+1}{n}}}\left[\overline{y}^{\frac{n+1}{n}} - \left(\frac{\overline{h}}{2}\right)^{\frac{n+1}{n}}\right]; \tag{18}$$

$$-\infty < \overline{x} \le -\overline{x_1}$$

$$\overline{u_2} = 1 - 2^{\frac{1}{n}}\left(\frac{4\,(2n+1)}{n+1}\right)\frac{\overline{g}}{\overline{h}^{\frac{2n+1}{n}}}\left[\overline{y}^{\frac{n+1}{n}} - \left(\frac{\overline{h}}{2}\right)^{\frac{n+1}{n}}\right]; \tag{19}$$

$$-\overline{x_1} \le \overline{x} \le \overline{x_2}$$

The normal load is given [19] as

$$w_y = \int_{-\infty}^{x_2} p\, dx \tag{20}$$

The dimensionless load $\overline{w_y} = \frac{W\alpha}{\sqrt{2Rh_0}}$ is calculated as

$$\overline{w_y} = \int_{-\infty}^{\overline{x_2}} \overline{x}\ \frac{d\overline{p}}{d\overline{x}}\, d\overline{x} \tag{21}$$

The tangential load is given [20] as

$$w_x = -2\int_{h_1}^{h_2} p\,dh \;=\; -2\,h_0\int_{-\infty}^{x_2} x^2\frac{dp}{dx}\,dx \tag{22}$$

The dimensionless load $\overline{w_x} = \frac{W_x\alpha}{2h_0}$ comes out to be

$$\overline{w_x} = \int_{-\infty}^{\overline{x_2}} \overline{x}^{\,2}\,\frac{d\overline{p}}{d\overline{x}}\,d\overline{x}. \tag{23}$$

The load $\overline{W}$ is calculated by

$$\overline{W} = \sqrt{\overline{w}_x^{\,2} + \overline{w}_y^{\,2}} \tag{24}$$

the surface traction force T_F, obtained from the integration of shear stress τ over the entire length, may be written as [20]

$$T_{Fh} \;=\; \int_{-\infty}^{x_2}\left(\frac{h}{2}\left(\frac{dp}{dx}\right)\right)\,dx \tag{25}$$

Then, the dimensionless traction may be written as

$$\overline{T_{Fh}} \;=\; \int_{-\infty}^{\overline{x_2}} \overline{h}\,\left(\frac{d\overline{p}}{d\overline{x}}\right)\,d\overline{x}\,; \tag{26}$$

Finally, one can get the consistency expression in the form

$$\overline{m} = \overline{m_0}\,\overline{E}. \tag{27}$$

3 Results and discussion

Two heavily loaded infinite rigid symmetric roller bearings are employed for the discussion. They are lubricated with non- Newtonian power law compressible fluid. In this setup the thermal effect of the fluid is beneath the rolling and normal motions. It is presumed that the lubricant pressure is a constant across the film thickness. At the same time, the consistency is licensed to differ exponentially with pressure and film temperature. The reshaped Reynolds and energy equations are derived and solved concurrently yielding pressure and temperature. The following values are used to the numerical calculations:

$-0.09 <$ q < 0.09; $0.4 \leq$ n ≤ 1.15; $\overline{T_0} = 3$; $\overline{\varepsilon} = 0.5$; $h_0 = 4\times10^{-6}$ m;

$\alpha = 0.6\times10^{-9}$ pa^{-1} m^2; $\overline{\gamma} = 5$; U $= 4$ m s^{-1} and $R = 0.03$ m.

This paper investigates to show the variation of consistency in a steady state thermal lubrication. The dimensionless velocity $\overline{u}$ pressure $\overline{p}$, temperature $\overline{T}$ are calculated as functions of the non Newtonian power law flow behavior index n and squeezing parameter q; & $\overline{m}$ is the consistency of the lubricant.

3.1 Pressure distribution

The pressure $\overline{p}$ against $\overline{x}$ for different values of q for a fixed n and for different values of n for a fixed q is shown respectively in Figs. 2 and 3 for compressible fluids in thermal case. From the graph, it is possibly known that $\overline{p}$ increases continuously in the input region and decreases in the outlet region. Once the pressure reaches the zenith, at the point of maximum pressure $\overline{x} = -\overline{x_1}$, $\overline{p}$ falls down, making a steep slope in graph and reduces to the ambient pressure $\overline{p_2} = 0$ [14, 21]. Also, the behavior of $\overline{p}$ against $\overline{x}$ for n (fixed) and different values of q are similar to that of Prasad et al. [17]. The lubricant pressure $\overline{p}$ increases significantly with n for a fixed value of q, particularly for $n \geq 1$. This is also similar with the results of Safar and Shawki [22]. Here it is noted that fixed q value gives both the points of cavitation and maximum pressure nearer to the centre line of contact, (the origin 0) as n increases. Fixed n value increases $\overline{p}$ considerably as q decreases; and the cavitation point moves slowly towards the centre line of contact as q increases. The change in pressure with respect to q accounts for the observation that as the surfaces approach each other, comparatively more pressure is generated. The comparison of pressure and density is presented in Fig. 4 and the compressibility for different values of n is presented in Fig. 5.

3.2 Temperature distribution

The temperature $\overline{T}$ verse $\overline{x}$ with respect to the different values of n is shown in Figs. 6 and 7. It is notable to understand that $\overline{T}$ increases in inlet area, and the increase in temperature is ceased at the maximum pressure point, $\overline{x} = -\overline{x_1}$ and then $\overline{T}$ comes down slowly to the outer region. The increase in $\overline{T}$ in the inner area is because of the dragging action of the faster layers in the high pressure region which

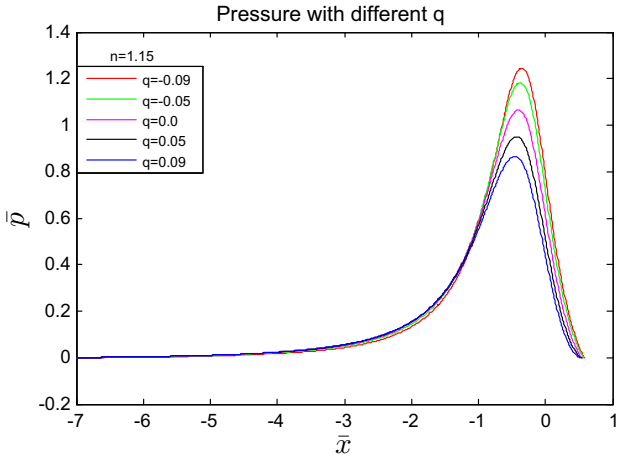

Fig. 2 $\overline{p}$ Vs $\overline{x}$

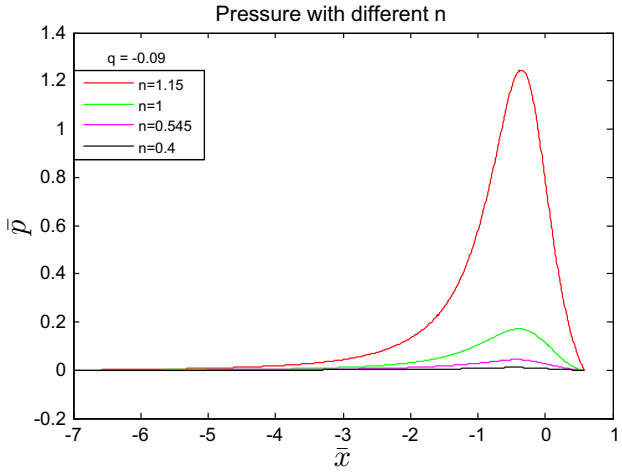

Fig. 3 $\bar{p}$ Vs $\bar{x}$

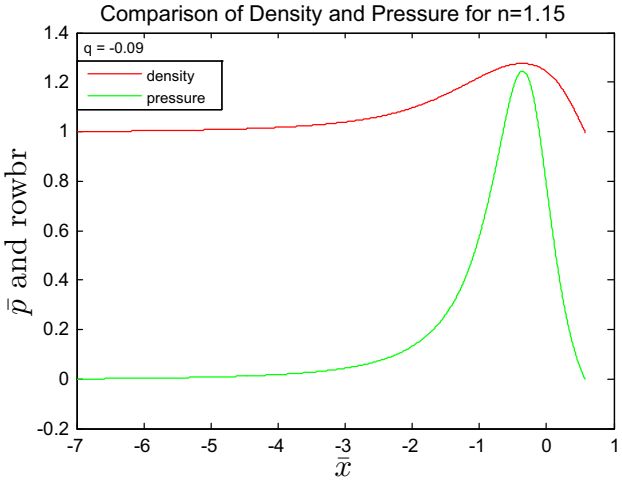

Fig. 4 $(\bar{p}$ & $\bar{\rho})$ Vs $\bar{x}$

makes more viscous dissipation in the convergence zone and results in more temperature [23]. From Figs. 6 and 7, it is learnt that $\overline{T}$ increases with n [24]. An increase in n denotes an enhanced effective viscosity. This increases the resistance to the motion, leading to a higher viscous dissipation. Similarly, $\overline{T}$ increases as q decreases with a fixed n.

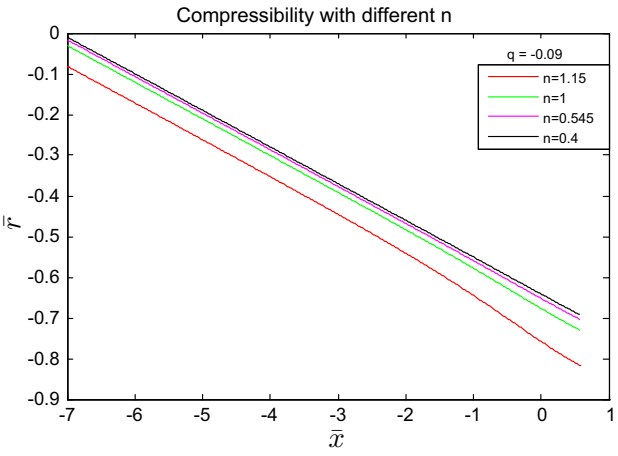

Fig. 5 $\bar{r}$ Vs $\bar{x}$

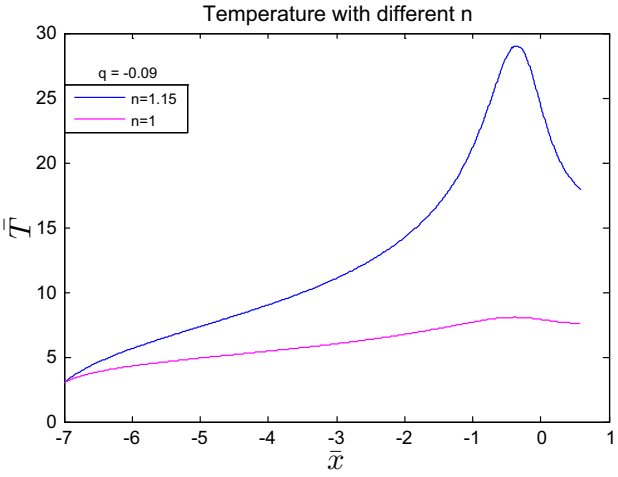

Fig. 6 $\overline{T}$ Vs $\bar{x}$

3.3 Load and traction

Load carrying capacity and traction force are the important features of bearings. It is presented in Table 1 which contains tangential and normal loads with different n and q values for thermal conditions. From the table it can be clearly stated that both the dimensionless load $\overline{W}$ and the dimensionless traction force $\overline{T}_F$ increases with n, but the normal load decreases with q which is in similar to the previous findings [19].

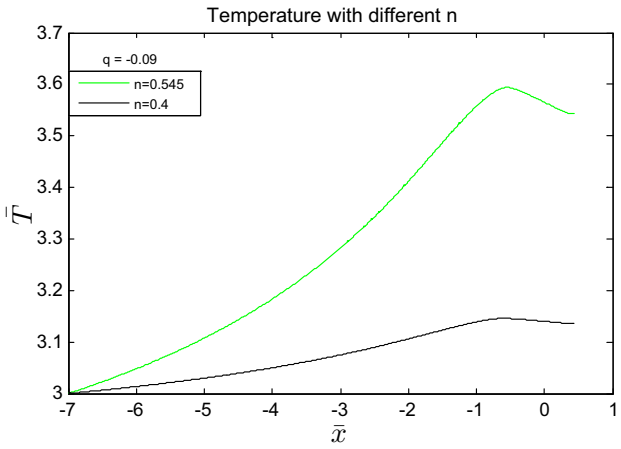

Fig. 7 $\overline{T}$ Vs $\bar{x}$

Table 1 Load and traction

	n/m_0	$q = -0.09$	$q = -0.05$	$q = 0.00$	$q = 0.05$	$q = 0.09$
Tangential load	1.15/0.56	2.420923	2.572450	2.596763	2.564392	2.518602
	1.00/0.75	0.489771	0.558945	0.575525	0.574329	0.566990
	0.545/86.0	0.173526	0.206755	0.213715	0.214810	0.214261
	0.40/128.0	0.048511	0.053794	0.054186	0.053736	0.053199
Normal load	1.15/0.56	1.590878	1.568511	1.470203	1.360181	1.269853
	1.00/0.75	0.263022	0.284669	0.279817	0.266758	0.253891
	0.545/86.0	0.075237	0.087509	0.087798	0.085190	0.081729
	0.40/128.0	0.019844	0.021254	0.020700	0.019967	0.019218
Load	1.15/0.56	2.896853	3.012926	2.984071	2.902791	2.820618
	1.00/0.75	0.555928	0.627260	0.639943	0.633256	0.621239
	0.545/86.0	0.189134	0.224511	0.231046	0.231086	0.229319
	0.40/128.0	0.052413	0.057841	0.058005	0.057326	0.056564
Traction	1.15/0.56	2.416422	2.572053	2.592239	2.557966	2.515180
	1.00/0.75	0.488843	0.558045	0.575231	0.574004	0.566903
	0.545/86.0	0.173212	0.205320	0.212583	0.213761	0.215418
	0.40/128.0	0.048604	0.054417	0.055018	0.054238	0.053598
Co-efficient of traction	1.15/0.56	0.834154	0.853673	0.868692	0.881209	0.891712
	1.00/0.75	0.879328	0.889655	0.898879	0.906432	0.912536
	0.545/86.0	0.915816	0.914519	0.920090	0.925026	0.939380
	0.40/128.0	0.927333	0.940802	0.948493	0.946129	0.947566

3.4 Consistency

The main and important feature of this paper is to study the variation in the consistency ($\overline{m}$) of the non Newtonian power law compressible fluids with pressure and the temperature as shown in the below figures. The overall consistency changes with $\bar{x}$ at different positions of the lubricant heights above the x-axis is shown in Fig. 8. This indicates basically the dominance of temperature over the pressure is in accordance with the result of Espejel [25]. A one dimensional consistency variation in $\overline{m}$ with $\bar{x}$ for different flow index n is given in Figs. 8 and 9. Hence, the consideration of the consistency variation with pressure and temperature is well justified.

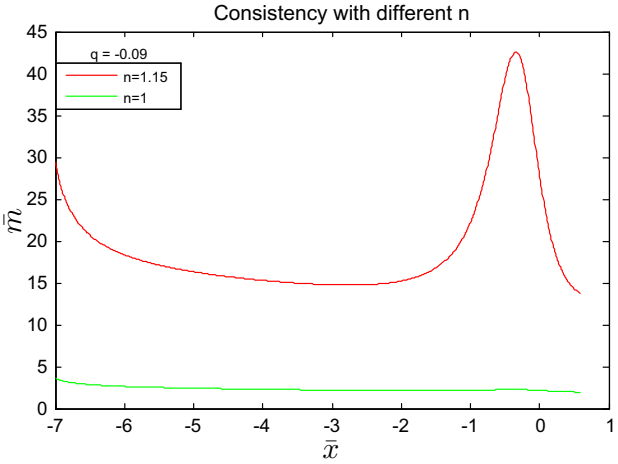

Fig. 8 $\overline{m}$ Vs $\bar{x}$

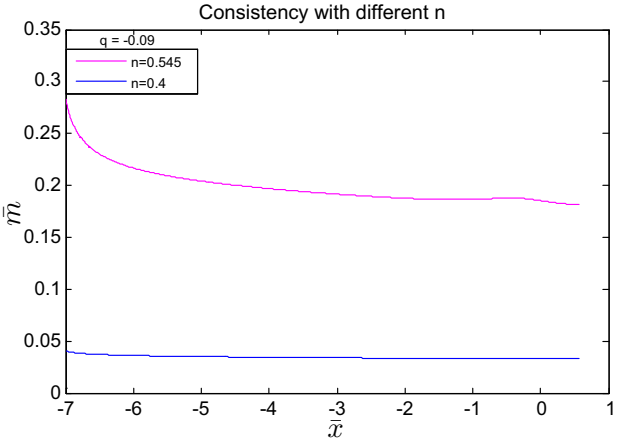

Fig. 9 $\overline{m}$ Vs $\bar{x}$

4 Conclusion

This problem consists the following aspects:

- The pressure and the temperature is considered to study the variation of lubricant consistency of the non Newtonian power law fluids with respect to the flow index n and the normal velocity q.
- A descriptive method is used to analyze the pressure and the temperature and hence the effects of them on the consistency m of the fluids.
- Loads and tractions are also included in the study of consistency variation.
- It is concluded that the pressure and the corresponding temperature increase with n and decrease as q increases numerically. Also the position of the pressure peak moves away from the centre line of contact as q increases.
- The load and the traction also follow the trend of pressure with q and n. These results are compared with the previous findings and are found to be in good agreement.

Compliance with ethical standards

Funding This study was not funded by any organizations.

Conflict of interest The authors declare that they have no conflicts of interest.

Ethical approval This article does not contain any studies with human participants or animals performed by any of the authors.

References

1. Mohd Yusof, Nural Farhana, and Zaidi Mohd Ripin. 2014. Analysis of Surface Parameters and Vibration of Roller Bearing. *Tribology Transactions* 57: 715–729.
2. Jakobsson, B., and L. Floberg. 1957. The finite journal bearingconsidering vaporization. *Transactions of Chalmers University of Technology* 3: 190.
3. Elrod, H.G., and M.L. Adams. 1974. A computer program for cavitation and starvation problems. In *Proceeding of the first Leeds-Lyon sumposium on tribology–cavittion and related phenomena in lubrication*, ed. D. Dowson, M. Godet, and C.M. Taylor, 37–41. England: University of Leeds.
4. Chevalier, F., A.A. Lubrecht, P.M.E. Cann, F. Colin, and G. Dalmaz. 1998. Film thickness in starved EHL point contacts. *Journal of Tribology* 120 (1): 126–33.
5. Lewy, H., and G. Stampacchia. 1969. On the regularity of solution of variational inequality. *Communications on Pure and Applied Mathematics* 22: 153–88.
6. Rohde, S.M., and G.T. Mc Allister. 1975. A variational formulation for a class of free boundary problems arising in hydro dynamic lubrication. *International Journal of Engineering Science* 13 (9–10): 841–50.
7. Cimatti, G. 1977. On a problem of the theory of lubrication governed by a variational inequality. *Applied Mathematics and Optimization* 3 (2–3): 227–42.
8. Strozzi, A. 1985. Formulation of three lubrication problems in terms of complementarity. *Wear* 104 (2): 103–19.
9. Kostreva, M. 1984. Elasto-hydrodynamic lubrication: a non-linear complementarity problem. *International Journal for Numerical Methods in Fluids* 4 (4): 377–97.
10. Oh, K.P. 1984. The numerical solution of dynamically loaded elasto hydrodynamic contact as a nonlinear complementarity problem. *Journal of Tribology* 106 (1): 88–95.
11. Oh, K.P., and P.K. Goenka. 1985. The elasto hydrodynamic solution of journal bearings under dynamic loading. *Journal of Tribology* 107 (3): 389–94.

12. Giacopini, M., M.T. Fowell, D. Dini, and A. Strozzi. 2010. A mass-conserving complementarity formulation to study lubricant films in the presence of cavitation. *Journal of Tribology* 132 (4): 041702.
13. Kushwaha, M., and H. Rahnejat. 2004. Transient concentrated finite line roller-to-race contact under combined entraining, tilting and squeeze film motions. *Journal of Physics D Applied Physics* 37 (14): 2018.
14. Hultqvist, Tobias, Mohammad Shirzadegan, Aleks Vrcek, Yannick Baubet, Braham Prakash, Pär Marklund, and Roland Larsson. 2018. Elastohydrodynamic lubrication for the finite line contact under transient loading conditions. *Tribology International* 127: 489–499.
15. Minewitsch, A.A. 2011. Some Developments in Triboanalysis of Coated Machine Components. *Tribology in Industry* 33 (4): 153–158.
16. Prasad, D., P. Singh, and P. Sinha. 1988. Non-uniform temperature in non-Newtonian compressible fluid film lubrication of rollers. *ASME Journal of Tribology* 110 (4): 653–658.
17. Prasad, D., S.V. Subrahmanyam, and S.S. Panda. 2014. Thermal, Squeezing and Compressibility Effects in Lubrication of Asymmetric Rollers. *Tribology in Industry* 36: 244–258.
18. Wei, Pu, Jiaxu Wang, and Dong Zhu. 2016. Friction and flash temperature prediction of mixed lubrication in elliptical contacts with arbitrary velocity vector. *Tribology International* 99: 38–46.
19. Prasad, D., and Venkata Subrahmanyam Sajja. 2016. Thermal Effect in non-Newtonian Lubrication of Asymmetric Rollers Under Adiabatic and Isothermal Boundaries. *International Journal of Chemical Sciences* 14: 1641–1656.
20. Prasad, D., Punyatma Sing, and Prawal Sinha. 1987. Thermal and squeezing effects in Non-Newtonian fluid film lubrication of rollers. *Wear* 119: 175–190.
21. Hajishafiee, A., A. Kadiric, S. Ioannides, and D. Dini. 2017. A coupled finite volume CFD solver for two dimensional EHL problems with particular application to rolling element bearings. *Tribology International* 109: 258–273.
22. Safar, Z.S., and G.S.A. Shawki. 1979. Performance of thrust bearing operating with non-Newtonian lubricating film. *Tribology International* 12: 31.
23. Gul, Taza, Imran Khan, Muhammad Altaf Khan, S. Islam, Tanaveer Akhtar, and S. Nasir. 2015. Unsteady Second order Fluid Flow between Two Oscillating Plates. *Journal of Applied Environmental and Biological Sciences* 5: 52–62.
24. Ma, Fangbo, Zhengmei Li, Shengchang Qiu, Baojie Wu, and Qi An. 2016. Transient thermal analysis of grease lubricated spherical roller bearings. *Tribology International* 93: 115–123.
25. Morales-Espejel, G.E., P.M. Lugt, H. Pasaribu, and H. Cen. 2014. Film thickness in grease lubricated slow rotating rolling bearings. *Tribology International* 74: 7–19.